Journal of Oil Palm Research Vol. 32 (1) March 2020 p. 124-138
DOI: https://doi.org/10.21894/jopr.2020.0012

CORROSION INHIBITION, ADSORPTION BEHAVIOUR AND THERMODYNAMIC PROPERTIES OF *N*-CINNAMALIDENE PALMITOHYDRAZIDE ON MILD STEEL IN HYDROCHLORIC ACID SOLUTION

NOOR KHAIRIN MOHD*; SHOOT-KIAN YEONG*; NOR AZOWA IBRAHIM; SITI MARIAM MOHD NOR**; CHUNG-HUNG CHAN*; SOOK-WAH TANG*; WEN-HUEI LIM* and ZAINAB IDRIS***

ABSTRACT

The corrosion inhibitory efficiency of N-*cinnamalidene palmitohydrazide (CPH) on mild steel in 1 M hydrochloric acid solution was studied using Tafel polarisation, electrochemical impedance spectroscopy and scanning electron microscopy-energy dispersive X-ray spectroscopy (SEM-EDX). Tafel polarisation analysis showed that the maximum inhibition efficiency (η_{Tafel}%) approached 95% in the presence of 200 mg litre^{-1} of CPH at 328K. The percentage inhibition efficiency increased with increasing inhibitor concentration and temperature of the test medium. Tafel polarisation study clearly revealed that CPH functions as a mixed-type inhibitor with a predominant anodic control. The adsorption of CPH on mild steel surface obeyed the Langmuir's adsorption isotherm. The evaluation of the thermodynamic and activation parameters indicated that the adsorption of CPH on the mild steel surface took place spontaneously through both physisorption and chemisorption with Gibbs free energy of adsorption (ΔG^{o}_{ads}) values from -34.33 kJ mol^{-1} to -41.38 kJ mol^{-1}. Impedance spectroscopy analysis showed that corrosion of mild steel in 1 M hydrochloric acid solution was mainly controlled by a charge transfer process and CPH formed a protective film on the metal-solution interface. The protective film was further confirmed by SEM images and the elemental analysis that measured by EDX analysis.*

Keywords: corrosion inhibitor, electrochemical analysis, inhibition efficiency, protective film, mild steel.

Date received: 5 December 2018; **Sent for revision**: 6 December 2018; **Accepted**: 24 March 2019.

INTRODUCTION

Mild steel is widely applied as the constructional materials for boilers, storage tanks, building constructions, reactors as well as oil and gas pipelines. Its broad applications and never-ending uses are due to its material properties that are accepted in various applications and price that relatively cheaper than other metals (Su *et al*., 2016). In general, mild steel is a ferrous metal with carbon content of approximately 0.05%-0.25% by weight. Meanwhile, acid solutions particularly hydrochloric acid are commonly used in industrial processes such as acid pickling of iron and steel; chemical cleaning and well acidification for oil and gas exploration. In these applications, acid is applied to clean metal surface and remove impurities such as stains, inorganic contaminants, corrosion products from ferrous metals. If these processes are carried out without an appropriate protection, the metal surfaces especially mild steel tends to get corroded. Once metal is exposed to acidic environment, corrosion may take place where it involves oxidation-reduction reaction. Furthermore, this

* Malaysian Palm Oil Board,
6 Persiaran Institusi, Bandar Baru Bangi,
43000 Kajang, Selangor, Malaysia.
E-mail: noorkhairin@mpob.gov.my

** Department of Chemistry, Faculty of Science,
Universiti Putra Malaysia, 43400 UPM Serdang,
Selangor, Malaysia.

acid-metal interaction can also lead to subsequent diffusion of hydrogen gas continuously into metal where it may gradually weaken the mechanical strength (Diblíková *et al.*, 2014). One of the best options of protecting the metallic surfaces against corrosion in the acidic environment is through use of corrosion inhibitors (Paul *et al*., 2012).

The selection of inhibitors is controlled by its economic availability, efficiency to inhibit the substrate material, safety and environmental side effects. Many types of corrosion inhibitors which include anodic, cathodic, oxygen scavenger and precipitates are extensively applied to control corrosion. However, a proportion of them particularly those containing chromate, nitrite and other heavy metals were found to be toxic and harmful to ecological system especially aquatic life. The use of these inhibitors is now being gradually restricted by various environmental regulations (Roy *et al*., 2014). Since the use of corrosion inhibitors is still one of the most practical techniques in combating corrosion, replacement of these inorganic inhibitors with green, non-toxic and safe chemicals is very crucial. These safety and environmental issues have encouraged people to use organic inhibitors in order to address the hazard of those toxic corrosion inhibitors. The effectiveness of organic inhibitors depends largely on the presence of heteroatoms such as sulphur, nitrogen, oxygen and/or multiple bonds (Verma and Quraishi, 2014; El-Maksoud, 2008). Previous studies reveal that several organic inhibitors include oxadiazoles (Chakravathy and Mohana, 2014), thiosemicarbazides (Ramya *et al*., 2015), Schiff bases (Singh and Quraishi, 2012; Ramesh and Adhikari, 2007), henna extract (Hamdy and El-Gendy, 2013) and 2-mercaptothiazoline (Solmaz *et al*., 2008) have shown good inhibition properties on various metallic surfaces in acidic media.

Schiff base compounds are effective corrosion inhibitors for corrosion of mild steel (Verma and Quraishi, 2014; Chitra *et al*., 2010; Desai *et al*., 1986), aluminium (Safak *et al*., 2012), copper (Li *et al*., 1999), nickel (Mishra *et al*., 2015) and zinc (Tawfik and Zaky, 2015) in acidic media like hydrochloric acid, nitric acid, sulphuric acid and phosphoric acid. The specific interaction between functionalities in Schiff base compounds with metal surface is a crucial part for the mechanistic performance of molecules (Chitra *et al*., 2010). Imine group in Schiff base molecules can act as an active centres for adsorption on the metal surfaces. This is commonly followed by formation of a protective layer that protects the surface from elements causing corrosion. Molecular weight, polarity, water miscibility, electron density, boiling point and melting point are important properties to be considered for selecting effective corrosion inhibitors.

The inhibitory activities of organic molecules are accomplished not only through adsorption of active centres alone but also could be supported by the presence of long-chain alkyl group. Schiff base with long-chain alkyl can be produced from nitrogen-based compounds derived from vegetable oils such as palm oil, soyabean oil, rapeseed oil and so forth. Malaysia as one of the world's largest palm oil producers and the growth of oleochemical industry sectors offers a great opportunity to apply palm-based sources for development of downstream products particularly corrosion inhibitors (Kushairi *et al*., 2018; Rafiquee *et al*., 2007). A new Schiff base compound namely, *N*-cinnamalidene palmitohydrazide (CPH) was synthesised from palmityl hydrazide and *trans*-cinnamaldehyde; and was applied for corrosion inhibitor. The inhibition properties of CPH were tested on corrosion of mild steel in acidic medium using electrochemical and surface analyses.

MATERIALS AND METHOD

Preparation of *N*-cinnamalidene Palmitohydrazide

A mixture of palmitate hydrazide, *trans*-cinnamaldehyde and dimethylformamide was charged into a two-necked reaction flask equipped with a condenser and a recirculating chiller. The reaction mixture was then heated at 90°C for 2 hr. After cooling to room temperature, the precipitates were filtered off under vacuum and recrystallised using dimethylformamide and water. Off-white solid product obtained from this one-pot synthesis was collected and dried in an oven for overnight. The CPH obtained was characterised by infrared spectroscopy (Nicolet Magna-IR 550 Spectrometer II), Nuclear magnetic resonance (NMR) spectroscopy (JEOL JNM ECZR 600MHz), mass spectroscopy (Agilent 5975C).

Electrochemical Measurement

The electrochemical measurements were performed using a three-electrode cell assembly potentiostat (Methrom Autolab PG 204, Netherlands) equipped with a 100-ml water-jacketed corrosion cell. Saturated silver/silver chloride (Ag/AgCl) in 3 M KCl and platinum were used as reference and counter electrodes, respectively. Mild steel specimens with an exposed area of 4.5 cm^2 were used as working electrode. The experiment was carried out under a non-stirred condition and the working electrode was immersed in the test solution at open circuit potential (OCP) for 30 min to attain a stabilised OCP before performing measurement.

Electrode and Solutions Preparation

Mild steel coupons of dimension 2.5 cm x 2.5 cm x 0.3 cm (wt. % composition: 0.32 Mn, 0.09 Cu, 0.07 C, 0.04 Cr, 0.03 Pb, 0.03 Ni, 0.02 Al and 0.01 S and the remainder is iron) were mechanically abraded with different grades of emery papers. The metal composition was measured using spark emission spectroscopy (Foundry-Master, Germany). The mild steel coupons were washed with distilled water, degreased with acetone and kept in a desiccator. This procedure was carried out prior to each experiment. The aggressive solutions of 1 M hydrochloric acid solution were diluted from 37% hydrochloric acid (AR grade, Merck Germany) using high-purity deionised water (resistivity ~ 18.2 MΩ.cm) that was obtained from a laboratory water purification system (ELGA, United Kingdom). Inhibited 1 M hydrochloric acid solutions were prepared by diluting inhibitor solution in alcohol with 1 M hydrochloric acid solution to obtain various concentrations: 25-200 mg litre^{-1}.

Electrochemical Impedance Spectroscopy

Electrochemical impedance spectroscopy was carried out to have a thorough understanding of the corrosion product film and inhibitor performance through electrochemical system. Impedance behaviour is commonly explained by pure electrical models that are used to verify and calculate the numerical values corresponding to the electrochemical system under examination. The measurement was performed at an open circuit potential in the frequency range from 100 kHz to 0.01 Hz with amplitude of 5 mV as excitation signal and scan rate of 1 mV s^{-1}. Data obtained was fitted with sets of equivalent circuits using NOVA software. The percentages of inhibition efficiency from impedance measurements were calculated using charge transfer resistance values as expressed by Equation (1):

$$\eta_{EIS}\,(\%) = \frac{R_{ct} - R'_{ct}}{R_{ct}} \times 100 \qquad (1)$$

where R_{ct} and R'_{ct} are the charge transfer resistances of working electrode in the absence and presence of inhibitor, respectively.

Tafel Polarisation

The Tafel polarisation measurements were started from cathodic to the anodic reactions (E =E_{corr} ± 250 mV, where E is potential and E_{corr} is corrosion potential) at a constant sweep rate of 1 mV s^{-1}. The low sweep rate was set to obtain a steady state current-potential curve (Rivera-Grau *et al*., 2013). The corrosion potential (E_{corr}) was observed when the electrode attained a steady state. A plot of potential, E against *log* i_{corr} (Tafel plot) was constructed and the linear Tafel segments of anodic and cathodic curves were extrapolated to obtain corrosion current density (i_{corr}) and E_{corr}. The corrosion rate (CR) and percentage of inhibition efficiency $\eta_{Tafel}(\%)$ was calculated using Equations (1) and (2) (Shahin *et al*., 2003).

$$\text{Corrosion rate, CR (mm yr}^{-1}) = \frac{0.129 \times \text{Eq. W} \times i_{corr}}{d} \qquad (2)$$

$$\text{Inhibition efficiency, } \eta_{Tafel}\% = \frac{(i'_{corr} - i_{corr})}{i'_{corr}} \times 100 \qquad (3)$$

where Eq.W and *d* are the equivalent weight (g) and density (g cm^{-3}) of the corroding metal, respectively. The i'_{corr} and i_{corr} are the corrosion current density values in blank and in the presence of inhibitors, respectively. Adsorption isotherm of CPH was calculated from linear polarisation measurement.

Surface Analysis

The mild steel coupons were exposed to 1 M hydrochloric acid solution containing CPH inhibitor with concentration of 200 mg litre^{-1} and also blank solution for 3 hr and 30 days before conducting surface morphological examination. After completion of immersion test, the coupons were removed from the solutions, rinsed with acetone and dried in an oven for 2 hr. The morphological analysis was performed using SEM-EDX spectrometry (JEOL JSM 6400, Japan).

RESULTS AND DISCUSSION

Characterisation of the CPH

CPH was synthesised with considerably good yield and purity of greater than 95%. CPH is white powder and it is soluble in dimethyl formamide, ethanol, isopropanol, dimethylsulfoxide and chloroform. The chemical data of CPH is shown as follows:

Off-white solid (yield: 98%, 0.9974 g); m.p.: 110.6°C-111.3°C; TLC (silica): R_f = 0.30 (eluent: petroleum ether-ethyl acetate, 8:2, v/v); υ_{max} (KBr, cm^{-1}) 3200 (N-H), 1667 (C=O), 1627 (C=N), 1570 (N-H), 1667 (C=C), 1187 (C-N), 722 (N-H); δ_H (500 MHz, $CDCl_3$) 9.75 (s, 1H, CONH), 7.64 (dd, 1H, *J* 5.75 Hz, NCHCH=CH), 7.46 (d, 2H, *J* 7.20 Hz, *o*-phenyl x 2), 7.34 (t, 2H, *J* 7.20 Hz, *m*-phenyl x 2), 7.30 (t, 1H, *J* 7.20

Hz, *p*-phenyl), 6.88 (d, 1H, *J* 1.8 Hz, NCHCH=CH), 6.88 (d, 1H, *J* 6.00 Hz, CH=CHPh), 2.67 (t, 2H, *J* 7.8 Hz, CH_2CO), 1.69 (m, 2H, CH_2CH_2CO), 1.34 (m, 24H, $(CH_2)_{12}CH_3$), 0.87 (t, 3H, *J* 7.20 Hz, CH_2CH_3); δ_C (125 MHz, $CDCl_3$) 176.5 (CO), 145.7 ($CHCH=CH$), 139.2 ($NCHCH=CH$), 136.0 (1C, $NCHCH=CH$), 129.0 (1C, $CCH=CH$), 128.9 (2C, phenyl), 127.1 (2C, phenyl), 124.9 (1C, phenyl), 32.6 (CH_2CO), 32.0 (CH_2CH_2CO), 29.8 (CH_2)10, 24.8 ($CH_2CH_2CH_3$), 22.8 (CH_2CH_3), 14.2 (CH_2CH_3); *m/z* (MS) 456 (M^+, $C_{28}H_{48}N_2OSi^+$).

Electrochemical Impedance Spectroscopy

The impedance measurements for mild steel in hydrochloric acid solution were carried out and data obtained are presented as Nyquist, phase and bode plots. A simple Randles CPE circuit consisting of solution resistance (R_s), charge transfer resistance (R_{ct}) and double layer capacitance (C_{dl}) as shown in *Figure 1a* was used in this study.

A constant phase element (CPE) was introduced instead of pure C_{dl} to describe roughness and inhomogeneity of the surface which gives more accurate fit. The impedance of CPE is expressed by Equation (4). The capacitance loop intersects the real axis at higher and lower frequencies. The intersect corresponds to R_s at high frequency and sum of R_s and R_{ct} at lower frequency. The value of R_{ct} is a measure of electron transfer across the surface.

$$Z_{CPE} = \frac{1}{Y_o(j\omega)^n} \quad (4)$$

where $j = \sqrt{(-1)}$, ω is the angular frequency in rad s^{-1}, Y_o is the constant of CPE element, n is an empirical constant that ranges from 0 to 1. When $n = 1$, the CPE performs as a pure capacitor, if $n = 0$, the CPE behaves as a pure resistor and if $n = 0.5$, the CPE is an equivalent of the Warburg element.

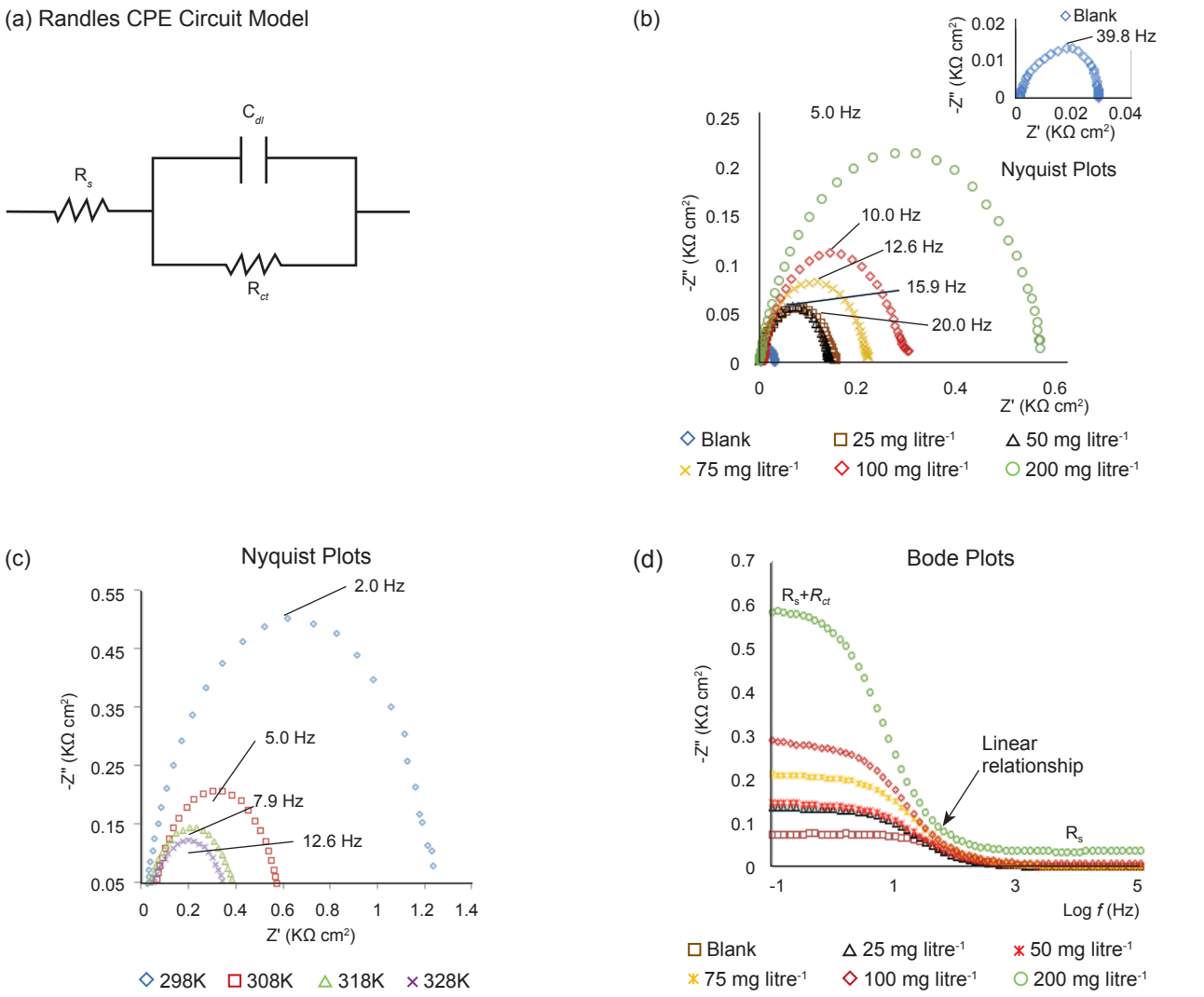

Figure 1. Randles constant phase element (CPE) Circuit Model (a) used to fit the experiment results, Nyquist plots for N*-cinnamalidene palmitohydrazide (CPH) on mild steel in 1 M hydrochloric acid solution with concentration range from 25 mg litre^{-1} to 200 mg litre^{-1} at 308K (b), and with concentration of 200 mg litre^{-1} at 298, 308, 318 and 328K (c), and Bode plots of CPH with concentration ranged from 25 to 200 mg litre^{-1} at 308K (d).*

Warburg element is a diffusion of ohmic species at the interface. The exponent of the CPE element can be used as a gauge for the heterogeneity or roughness of the surface and *f* is the frequency of sinusoidal perturbation signal in Hz. The correction in the capacitance to its real value is calculated using Equation (5).

$$C_{dl} = \frac{1}{(2\pi f_{max} R_{ct})} \quad (5)$$

where f_{max} is the frequency at which the imaginary component of impedance is maximum and R_{ct} is obtained from the parametric fit of the experimental spectrum to the equivalent circuit equation. The C_{dl} at the metal-interface is due to diffusion of soluble species.

Nyquist plots of mild steel in hydrochloric acid solution with the absence and the presence of various concentrations of CPH inhibitor are given in *Figure 1b*. It is evident from the Nyquist plots that the plots comprise of single capacitive loops. These single capacitive loops suggest that the corrosion of mild steel in 1 M hydrochloric acid solution is mainly controlled by a charge transfer process (El-Lateef, 2015). The charge transfer step dictates the rate of corrosion and the reaction is completely kinetic controlled. The shape of Nyquist plots obtained from mild steel in inhibited hydrochloric acid solutions are similar to that of blank solution indicating CPH inhibitor did not change the corrosion mechanism. The depressed semi-circles of Nyquist plots are often attributed to the surface roughness, inhomogeneity of the solid surface and adsorption of the inhibitor on the mild steel surface (Amin *et al*., 2007). It should also be noted that the peaks of the Nyquist plots are not located at the same frequencies of the apexes of the Nyquist plots.

The Nyquist plot of mild steel obtained in blank 1 M hydrochloric acid solution exhibits the smallest capacitive loop. Then, the presence of CPH at 25 mg litre^{-1} in test solution has given rise to the size of capacitive loop. This was due to formation of double layer capacitance at metal-solution interface that reduced the corroding process. Significant enlargement of the capacitive loops was observed when the inhibitor concentration was increased up to 200 mg litre^{-1}. Increase of inhibitor concentration has led to significant rise of thickness of the double layer capacitance. Meanwhile, reduce in size of capacitive loops was observed when the temperature was raised fro m 298K to 328K (*Figure 1c*) with R_{ct} values decreased from 1199 Ω cm^2 to 308 Ω cm^2 (*Table 1*) for mild steel in inhibited hydrochloric acid solutions. The same reduction trend was also found for mild steel in in blank solution with a similar ascending temperature. The R_{ct} values decreased from 116 Ω cm^2 to 21 Ω cm^2 as the temperature raised up to 328K. The smallest capacitive loop that lies on the experiment carried out at 328K implies that the corrosion process accelerated at higher temperature. According to Nyquist plots and R_{ct} values obtained, it can be concluded that CPH inhibitor has shown inhibitory action towards mild steel in hydrochloric acid solution and was still capable of reducing corrosion process even though the temperature was raised up to 328K.

TABLE 1. R_{ct} VALUES FOR MILD STEEL IN 1 M HYDROCHLORIC ACID SOLUTION (blank) AND 1 M HYDROCHLORIC ACID SOLUTION CONTAINING CPH AT DIFFERENT TEMPERATURES

Temperature (K)	R_{ct} (Ω cm^2)	
	1 M hydrochloric acid with presence of 200 mg litre^{-1} CPH	1 M hydrochloric acid without inhibitor (blank)
298	1 199	116
308	519	110
318	338	26
328	308	21

Note: CPH - *N*-cinnamalidene palmitohydrazide.

Bode plots of mild steel in 1 M hydrochloric acid solution containing different concentrations of CPH inhibitor at 308K are shown in *Figure 1d*. At low frequency, the presence of CPH inhibitor has enhanced the absolute impedance that confirmed the protection by inhibitor, which was attributed to the adsorption of the inhibitor molecules on the mild steel surface. A large plateau is ascribed to the corrosion of mild steel. A linear relationship between Z″ *vs.* log *f* that is observed at the intermediate frequencies suggesting formation of a protective film on the mild steel surface and the protective film has changed the electrode interfacial structure (El-Lateef, 2015; Tan *et al*., 1996; Sakunthala *et al*., 2013). The inhibition behaviour can be explained by the structure of electrical double layer where capacitor lies between metal and the outer Helmholtz plane; and the Gouy-Chapman diffuse layer (Sigircik *et al*., 2016). The electrochemical impedance parameters derived from the Nyquist plots are listed in *Table 2*.

It is clear that the impedance response of mild steel in blank solution has tremendously changed after adding CPH inhibitor. The R_{ct} value obtained for blank was lower than that with presence CPH inhibitor. Increase of R_{ct} values signifies a reduction in corrosion rate due to formation of adsorbed protective film on the metal-solution interface (Bentiss *et al*., 2007). From the results obtained, the mild steel behaves like a pure capacitor in the hydrochloric acid solution as constant, *n* values are very close to one. Notable decrease in C_{dl} values from 57.4-48.1 μF cm^{-2} was also observed with addition

of CPH inhibitor. This could be attributed to the decrease in local dielectric constant (ε_r) and increase in thickness of the electrical double layer (*d).* This phenomenon can be further understood using the Helmholtz model as shown by Equation (6).

$$C_{dl} = \frac{A\varepsilon_o \varepsilon_r}{d} \quad (6)$$

where ε_o is the permittivity of free space, ε_r is the local dielectric constant of the protective layer, *d* is the layer thickness and *A* is the surface area. In this model, C_{dl} is inversely proportional to surface change. The replacement of water molecules (water has high dielectric constant) with relatively smaller dielectric constant of inhibitor molecules has decreased the ε_r (Ozcan *et al*., 2008). On top of that, increase in thickness of the double layer at metal-solution interface has gradually reduced the C_{dl} values. This provides experimental evidence of adsorption of the CPH molecule on the mild steel surface (Li *et al*., 2008). The adsorption of inhibitor also prevented the extent of the metal dissolution (Rafiquee *et al*., 2007). A remarkable rise of the inhibition efficiency, η_{EIS} (%) was observed when concentration of inhibitor and temperature were increased (*Figure 2*). A maximum of 93.8% of inhibition efficiency was achieved for mild steel in the test solution containing 100 mg litre^{-1} CPH at 328K.

Tafel Polarisation

Polarisation measurements were carried out to understand the inhibitive characteristic which include anodic and cathodic reactions as well as inhibition efficiency of the studied inhibitor. CPH inhibitor with concentration in the range of 25-200 mg litre^{-1} in 1 M hydrochloric acid solution was tested for corrosion inhibitory properties. Typical Tafel polarisation curves of *Log i* against potential (E *vs*. Ag/AgCl) for mild steel in the absence and presence of different concentration of CPH at 308K were plotted as shown in *Figure 3*.

It was observed that similar shape of Tafel plots were obtained for mild steel in 1 M hydrochloric acid with the absence or presence of inhibitor indicating CPH inhibitor did not change the corrosion mechanism of mild steel. In the presence of inhibitor, both anodic and cathodic curves shifted to lower current densities, which reflects the inhibitory effect on both anodic and cathodic parts of polarisation curves. This indicates that CPH reacts as a mixed-type inhibitor (Negm *et al*., 2011; Bentiss *et al*., 2009). The shift could be attributed to the adsorption of the CPH inhibitor over the mild steel surface. In acidic solution, metal dissolution forms metal ions at anode and evolution of hydrogen gas from hydrogen ions occurs at the cathode. In inhibited acidic solution, CPH formed a barrier and reduced the corrosion rate by blocking both anodic and cathodic reactions on mild steel surface.

TABLE 2. IMPEDANCE PARAMETERS FOR CORROSION OF MILD STEEL IN 1 M HYDROCHLORIC ACID SOLUTION IN THE ABSENCE (blank) AND PRESENCE OF CPH AT 308K

Sample	*Rs* (Ω cm^2)	R_{ct} (Ω cm^2)	*n*	C_{dl} (μF cm^{-2})	CPE, Y_o (μS sα cm^{-2})
1 M hydrochloric acid without inhibitor (blank)	1.43	110.3	0.999	57.4	69.95
1 M hydrochloric acid with 200 mg litre^{-1} CPH	3.78	519.0	0.998	48.1	61.60

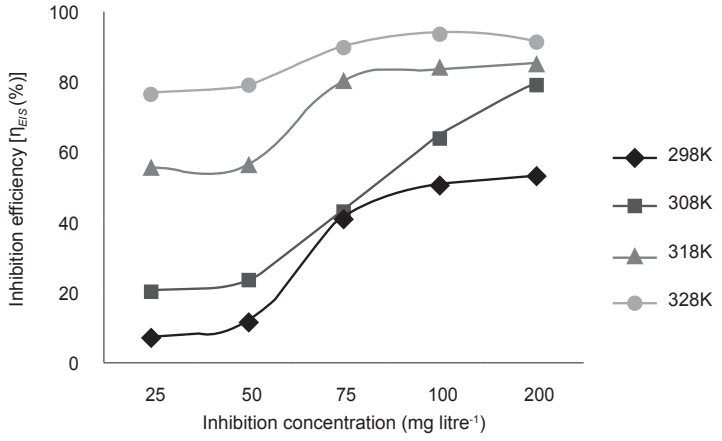

Figure 2. Inhibition efficiency, η_{EIS} (%) of N-*cinnamalidene palmitohydrazide (CPH) on mild steel in 1 M hydrochloric acid solution with concentration in range of 25-200 mg litre^{-1} at 298, 308, 318 and 328K obtained from linear polarisation analysis.*

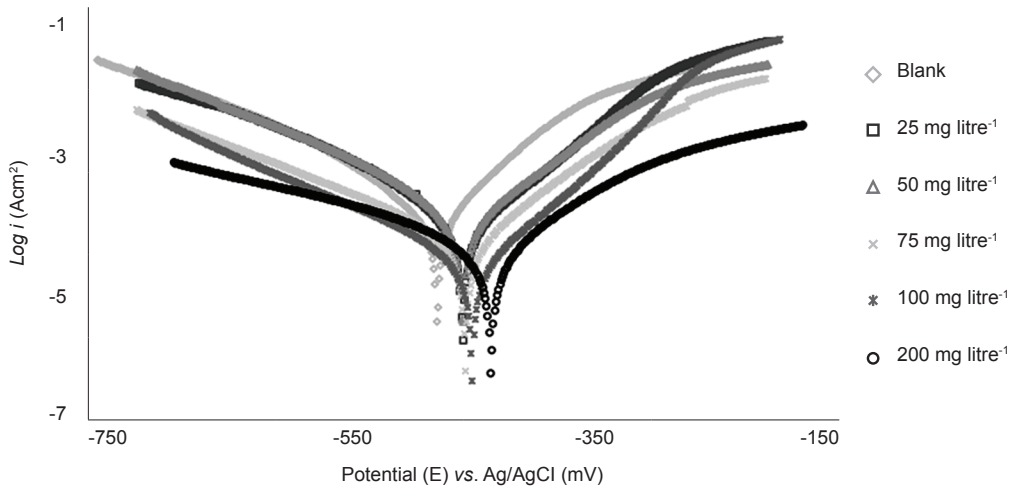

Figure 3. Tafel polarisation curves of mild steel in 1 M hydrochloric acid solution in the absence (blank) and presence of N*-cinnamalidene palmitohydrazide (CPH) ranged from 25-200 mg litre^{-1} at 308K.*

TABLE 3. ELECTROCHEMICAL POLARISATION PARAMETERS FOR MILD STEEL IN 1 M HYDROCHLORIC ACID SOLUTION IN THE PRESENCE OF CPH WITH DIFFERENT CONCENTRATIONS AT 308K

Concentration (mg litre^{-1})	E_{corr} (mV)	i_{corr} (μA cm^{-2})	β_a	β_c	CR mm yr^{-1}
Blank	-452	289.48	125.7	85.83	3.36
25	-435	86.39	99.3	63.2	1.00
50	-433	84.87	71.8	75.1	0.98
75	-430	83.13	62.7	66.2	0.97
100	-431	56.34	60.2	61.1	0.65
200	-411	34.59	44.3	39.0	0.40

Note: CPH - *N*-cinnamalidene palmitohydrazide.
CR - corrossion rate.

The Effect of CPH Concentration

The increase in CPH inhibitor concentration has resulted in gradual shifts of both anodic and cathodic curves towards lower current densities as shown in *Figure 3*. The CPH inhibitor has formed a barrier that blocked the mild steel surface from both anodic and cathodic reactions. The barrier has successively reduced the surface coverage for the subsequent surface reactions and this has led to decrease of current densities (Keersmaecker *et al*., 2014). It is evident from *Table 3* that the presence of CPH inhibitor has reduced E_{corr} value and a significant reduction of E_{corr} values was observed with increasing inhibitor concentrations.

Generally, the inhibitory action of an inhibitor can be classified exclusively as cathodic or anodic if the shift of E_{corr} with respect to E_{corr} of blank solution is at least -85 mV or +85 mV, respectively (Li *et al*., 2009; Verma and Quraishi, 2014). In the present study, the maximum shift of E_{corr} is only 41 mV, suggesting CPH acts as a mixed-type inhibitor with a predominant anodic control. A closer observation also reveals a slight change in both the Tafel slopes: β_a and β_c upon addition of the inhibitor. The presence of the inhibitor has significantly influenced kinetic of metal dissolution and hydrogen evolution processes. In the absence of inhibitor, the i_{corr} and CR values were found to be 289.48 μA cm^{-2} and 3.36 mm yr^{-1}, respectively. However, the presence of CPH at 25 mg litre^{-1} has effectively reduced the i_{corr} and CR values to 86.39 μA cm^{-2} and 1.00 mm yr^{-1}, respectively. Further increase in the inhibitor concentrations has led to dramatic decreases of these values. The lowest values of i_{corr} and CR were noticed at the inhibitor solution of 200 mg litre^{-1}. This may be attributed to greater surface coverage achieved at higher concentration. Remarkable increase of inhibition efficiency, η_{Tafel} (%) values was taking place notably with rise of the CPH inhibitor concentration (*Figure 4*). Increase in concentration allows more interaction of the inhibitor with metal surface thus improved surface coverage.

It is also seen that percentage of inhibition efficiency values calculated from both Tafel and impedance spectroscopy techniques gave similar trend upon increase concentration of inhibitor and temperature. However, values obtained from

impedance spectroscopy were slightly lower than that of Tafel technique. A prominent increase of η_{Tafel} (%) values up to a maximum of 94.9% was also observed when the temperature has been risen from 298K to 328K (*Figure 5*). The greater inhibitory action achieved at 328K could be associated with dispersibility of inhibitor in the test medium. As such, greater number of CPH molecules participated in the adsorption process.

Thermodynamic Parameters

The dependence of the CR on the temperature is expressed by the Arrhenius [Equation (7)] and Arrhenius transition state equation [Equation (8)] as follows:

$$\text{Arrhenius: } ln\ \text{CR} = \left(\frac{-\Delta E_a}{R}\right)\left(\frac{1}{T}\right) + A \qquad (7)$$

$$\text{Arrhenius transition state: } ln\left(\frac{C_R}{T}\right) = \left[\ln\left(\frac{R}{Nh}\right) + \frac{\Delta S_a}{R}\right] - \left(\frac{\Delta H_a}{RT}\right) \qquad (8)$$

where ΔE_a is the activation energy in J mol^{-1}, A is the electrochemical constant, R is the gas constant, T is the absolute temperature in Kelvin, E_a is the activation energy, ΔH_a is the entalphy of activation and ΔS_a is the entrophy of activation. The graphs of *ln* CR against 1/T x 1000 (K^{-1}) of mild steel of blank and inhibited 1 M hydrochloric acid gave straight lines (*Figure 5a*) and ΔE_a values were obtained from the slopes of the graphs. Meanwhile, plots of *ln* (CR/T) against 1000 x 1/T (*Figure 5b*) which also gave straight lines with slopes (ΔH_a/R) and intercepts [*ln*(R/Nh) + ΔS_a/R] were established to obtain ΔH_a and ΔS_a values, respectively.

TABLE 4. ACTIVATION PARAMETERS FOR THE CORROSION OF MILD STEEL IN 1 M HYDROCHLORIC ACID SOLUTION CONTAINING DIFFERENT CONCENTRATIONS OF CPH

Sample	Concentration (mg litre^{-1})	E_a (kJ mol^{-1})	ΔH_a (kJ mol^{-1})	ΔS_a (J mol^{-1} K^{-1})
Blank	-	58.51	55.91	-53.94
	25	30.27	27.65	-156.92
	50	24.54	21.94	-174.48
CPH	75	24.38	21.78	-176.58
	100	34.42	31.82	-147.39
	200	31.42	28.82	-160.22

Note: CPH - *N*-cinnamalidene palmitohydrazide.

Data in both graphs reveals that the apparent ΔE_a values (*Table 4*) for inhibited 1 M hydrochloric acid solutions are significantly lower than that of blank solution. This suggests that the adsorption of the CPH molecules on the mild steel surface predominantly occurred through chemical adsorption leading to the formation of adsorptive films (Ramya *et al*., 2015; Zarrouk *et al*., 2011). The data also reveals that the ΔH_a values for dissolution of mild steel in hydrochloric acid in the presence of CPH inhibitor are lower (from 21.78 kJ mol^{-1} to 28.82 kJ mol^{-1}) than that in the absence of inhibitor (55.91 kJ mol^{-1}). Values of ΔH_a are all positive which are much related to the endothermic nature of the metal dissolution process (Singh and Quraishi, 2012). Data on entropy revealed that the sign of ΔS_a was negative which indicates that the formation of an activated complex in the rate determining step represents an association rather than a dissociation step. A decrease in disorderliness takes place during the course of the transition from reactants to activated complex (Ramesh and Adhikari, 2007).

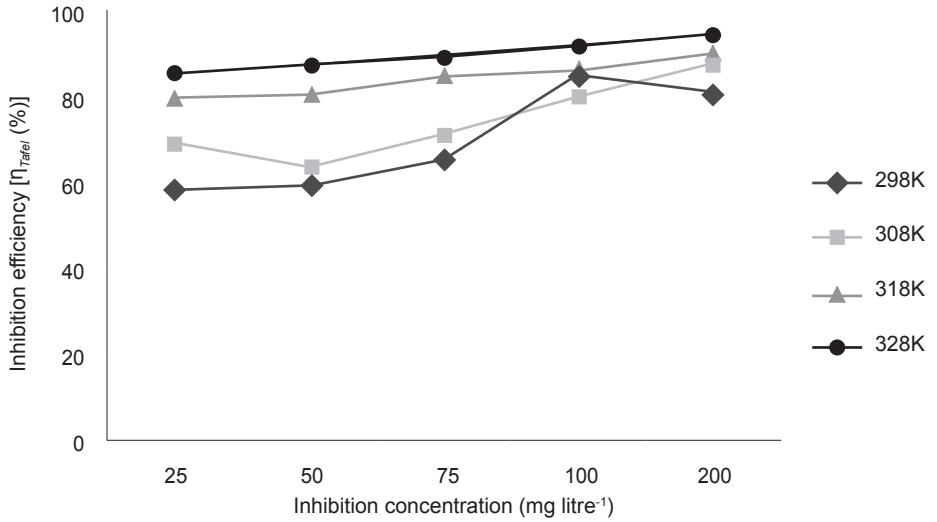

Figure 4. Inhibition efficiency, η_{Tafel} (%) of N-*cinnamalidene palmitohydrazide (CPH) on mild steel in 1 M hydrochloric acid solution with different concentrations at 298, 308, 318 and 328K obtained from impedance spectroscopy analysis.*

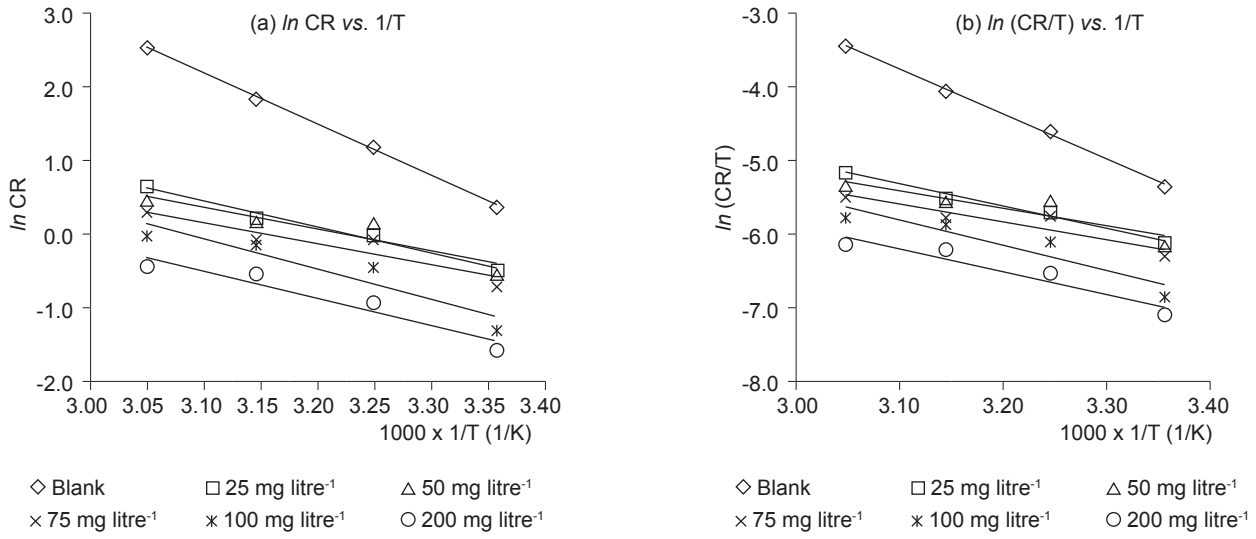

Figure 5. Plots of ln corrossion rate (CR) against 1/T x 1000 K^{-1} (a) and ln CR/T against 1/T x 1000 K^{-1} (b) for mild steel in 1 M hydrochloric acid solution with the absence (blank) and presence of 200 mg $litre^{-1}$ N-cinnamalidene palmitohydrazide (CPH).

Adsorption Isotherm and Free Energy of Adsorption

The mechanism of corrosion inhibition by CPH molecule may be explained on the basis of the adsorption behaviour. Information on the adsorption behaviour of inhibitor over metal surface can be obtained using the adsorption isotherms. Nature of testing media, chemical structure of inhibitors, charge distribution, and nature of metal primarily influence the adsorption of organic inhibitors on metal surface (Ehsani *et al*., 2014). Basically, the adsorption of an organic inhibitor at metal-solution interface can be presented as a substitution adsorption process between the organic molecules in aqueous solution $Org_{(sol)}$ and the water molecules on metallic surface $H_2O_{(ads)}$ as shown by Equation (9).

$$Org_{(sol)} + nH_2O_{(ads)} \longleftrightarrow Org_{(ads)} + nH_2O_{(sol)} \quad (9)$$

where, $Org_{(sol)}$ and $Org_{(ads)}$ are the organic molecules in the solution and adsorbed on the metal surface, respectively and *n* is the number of water molecules. Theoretically, the adsorption of inhibitor on corroding surfaces would not reach the real equilibrium but tends to become a quasi-equilibrium state when the rate of corrosion is sufficiently small. The quasi-equilibrium state is related to thermodynamic using appropriate equilibrium isotherms (Ghazoui *et al.*, 2012). In this study, surface coverage (θ) values that were obtained from linear polarisation analysis were fitted with several isotherms such as Temkin, Frumkin, Langmuir and Freudlinch. The adsorption behaviour of CPH inhibitor on the mild steel surface is best described by the Langmuir type adsorption. The Langmuir's adsorption isotherm, θ is related to the concentration of the inhibitor as given by Equation (10).

$$\frac{C_{inh}}{\theta} = \frac{1}{K_{ads}} + C_{inh} \quad (10)$$

where C_{inh} is the concentration of the inhibitor, θ is the fractional surface coverage and K_{ads} is the adsorption equilibrium constant obtained from the intercept of the straight line. The plots of C_{inh}/θ against C_{inh} gave straight lines with linear regressions, r^2 were close to one. The K_{ads} is related to the Gibbs free energy of adsorption (ΔG^o_{ads}) as described by Equation (11).

$$\Delta G^o_{ads} = -RT \ln (55.5\ K_{ads}) \quad (11)$$

where the *R* is the universal gas constant (R= 8.31446 J K^{-1} mol^{-1}), *T* is absolute temperature (K) and the value of 55.5 represents the molar concentration of water in solution expressed in unit of mol $litre^{-1}$ (El-Lateef, 2015). *Table 5* shows thermodynamic parameters including $ln\ K_{ads}$, ΔG^o_{ads}, H^o_{ads} and ΔS^o_{ads}.

It can be seen that $ln\ K_{ads}$ values increase with increasing temperature from 298K to 328K. Such behaviour can be interpreted on the basis that increase in temperature has allowed more adsorption of CPH molecules on the metal surface. The negative values of ΔG^o_{ads} signify a spontaneity adsorption of the CPH inhibitor on the mild steel surface (Solmaz

TABLE 5. THE LANGMUIR ADSORPTION ISOTHERM AND THERMODYNAMIC PARAMETERS FOR CPH ON MILD STEEL SURFACE IN 1 M HYDROCHLORIC ACID AT DIFFERENT TEMPERATURES

Temp. (K)	Equation	r^2	$In\ K_{ads}$ (L mol^{-1})	ΔG^o_{ads} (kJ mol^{-1})	ΔH^o_{ads} (kJ mol^{-1})	ΔS^o_{ads} (J mol^{-1}K^{-1})
298	y=1.1127x + 20.47	0.9815	9.84	-34.33	-40.47	249.8
308	y=1.0537x + 19.11	0.9908	9.91	-35.66		
318	y=1.0724x + 6.92	0.9994	10.92	-39.50		
328	y= 1.0295x + 5.49	0.9994	11.16	-41.38		

Note: CPH - *N*-cinnamalidene palmitohydrazide.

et al., 2008). Generally, values of ΔG^o_{ads} up to -20 kJ mol^{-1} are consistent with physisorption, while those around -40 kJ mol^{-1} or higher implies strong adsorption of inhibitor molecules on the mild steel surface through co-ordinate type bond or also known as chemisorption (Solmaz *et al*., 2008). In the present work, the calculated values of ΔG^o_{ads} at 298, 308, 318 and 328K were -34.33, -35.66, -39.50 and -41.38 kJ mol^{-1} respectively. This suggests that the adsorption of CPH inhibitor is not merely physisorption or chemisorption but involves both physisorption and chemisorption comprehensively. The adsorption of inhibitor accomplished with physisorption at 298K and 308K but approaching chemisorption at 318K and 328K.

Theoretically, the physisorption is an electrostatic interaction that occurs between charged molecules and charged metal surface. Chemisorption is related to charge share or charge transfer from inhibitor molecules to the mild steel surfaces (Bahrami and Hosseini, 2012). Physisorption could also take place at the initial stage of adsorption process (Solmaz *et al*., 2008). The enthalpy of adsorption can be calculated from Gibss-Helmholtz equation ($\Delta G^o_{ads} = \Delta H^o_{ads} - T\Delta S^o_{ads}$). The adsorption process was favourable through the displacement of water molecules from the mild steel surface.

Plot of ΔG^o_{ads} against T gave entalphy of adsorption (ΔH^o_{ads}) and the standard entropy (ΔS^o_{ads}) according to the thermodynamic equation. The plots gave a good dependence of ΔG^o_{ads} on T with linear equation of y = -0.2498x + 40.47 and r^2 of 0.967 indicating the adsorption of inhibitors is in good correlation with thermodynamic parameters. Basically, the negative value of the entalphy of adsorption ($\Delta H^o_{ads}<0$) is consistent with an exothermic process that involves either physisorption or chemisorption. While the positive value ($\Delta H^o_{ads}>0$) is related to an endothermic process through chemisorption (Durnie *et al*., 2001). The positive values of ΔH^o_{ads} signify a strong adsorptive activity of inhibitors onto the mild steel surface. In the present study, the negative value of ΔH^o_{ads} indicates the exothermic behaviour of adsorption by CPH on the mild steel surface. The positive value of standard entropy (ΔS^o_{ads}) suggests a random arrangement during the adsorption of inhibitor at the metal-solution interface (Benerjee and Malhotra, 1992).

Surface Analysis

SEM analysis. The SEM micrograph of the polished mild steel coupon (*Figure 6a*) shows a smooth surface that is free from any pit or tear. However, parallel lines on the mild steel surface are attributed to polishing scratch that are visible at micro scale. After exposing to test solution for 3 hr (*Figure 6b*), the mild steel surface appeared to be moderately rough. The appearance of parallel lines indicates that the surface is free from formation of protective layer and the surface is having direct contact with corrosive solution. The surface entirely suffers from severe corrosion after exposing to test solution for 30 days. Flakes-type corrosion products found on the mild steel (*Figure 6c*) could be due to continuous dissolution of iron and an attack of corrosive species. Indirectly, these results also revealed that the test solution was an appropriate medium for this investigation. After exposing the mild steel coupon in the test solution containing CPH for 3 hr, the surface appeared to be slightly rough due to an aggressive attack of the corrosive solution (*Figures 6d* and *6e*). The disappearance of scratch lines could be correlated to the formation of the protective layer but still incomplete. A smooth surface obtained after 30 days of immersion (*Figures 6f* and *6g*) might be attributed to the adsorption of inhibitor and formation of a protective layer on the surface. Some deposited particles that were found on the mild steel surface could be due to a multiple nucleation of inhibitor on the same site (Karthikaiselvi and Subhashini, 2014). These results also revealed that CPH inhibited mild steel surface through formation of a protective layer.

Energy dispersive X-ray spectroscopy (EDX) analysis. The EDX analysis was conducted to determine the elements on the mild steel surface

TABLE 6. QUANTITATIVE SEM-EDX DATA FOR POLISHED MILD STEEL AND MILD STEEL AFTER IMMERSED IN 1 M HYDROCHLORIC ACID SOLUTION IN THE ABSENCE AND THE PRESENCE OF CPH AT ROOM TEMPERATURE

Condition	Sample	Composition (%)			
		C	Cl	O	Fe
Before immersion	Polished mild steel	7.47	ND*	ND*	92.15
	1 M HCl with 200 mg litre^{-1} CPH	9.59	ND*	ND*	90.41
After 3 hr	1 M HCl without inhibitor	9.78	ND*	ND*	90.22
	1 M HCl with 200 mg litre^{-1} CPH	10.72	ND*	7.92	81.04
After 30 days	1 M HCl without inhibitor	13.09	10.93	54.31	19.71

Note: *ND - not detected.
HCl - hydrochloric acid.
CPH - *N*-cinnamalidene palmitohydrazide.

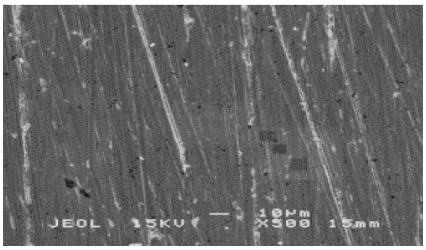

(a) Polished mild steel

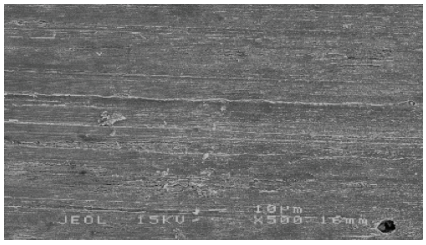

(b) Mild steel in 1 M HCl/ 3 hr
Magnification: 500X

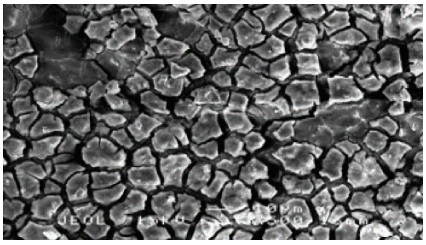

(c) Mild steel in 1 M HCl/ 30 days
Magnification: 500X

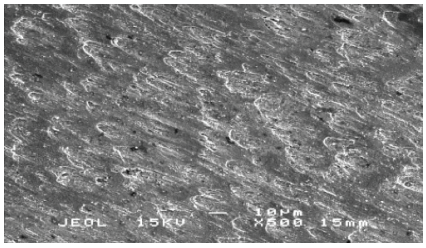

(d) Mild steel in inhibited 1 M HCl/ 3 hr
Magnification: 500X

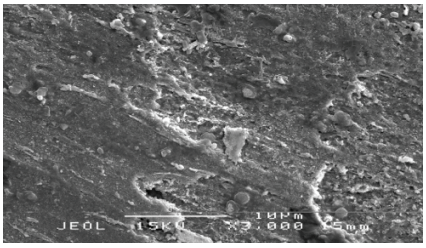

(e) Mild steel in inhibited 1 M HCl/ 3 hr
Magnification: 3000X

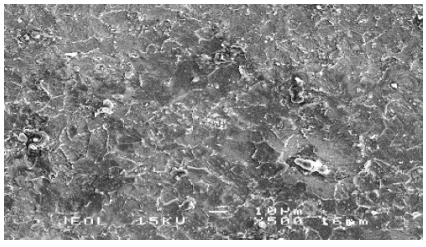

(f) Mild steel in inhibited 1 M HCl/ 30 days
Magnification: 500X

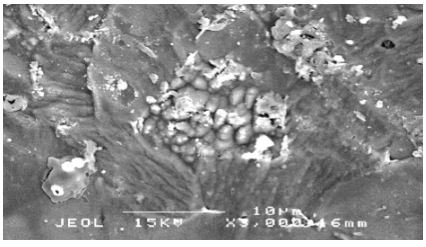

(g) Mild steel in inhibited 1 M HCl/ 30 days
Magnification: 3000X

Figure 6. Scanning electronic microscopy (SEM) images of a polished mild steel coupon (a), mild steel coupons after immersing in 1 M hydrochloric acid solution for 3 hr (b), and 30 days (c), mild steel coupons after exposing to 1 M hydrochloric acid solution containing 200 mg litre^{-1} CPH for 3 hr under 500X (d) and 3000X (e) magnifications; and 30 days under 500X (f) and 3000X (g) magnifications. Images 6a, 6b and 6c are reproduced from Mohd et al. *(2017) for comparison purpose.*

before and after immersion test. Polished mild steel coupon and mild steel coupons that were immersed in 1 M hydrochloric acid solution with the absence (blank) and presence of 200 mg litre^{-1} CPH for 3 hr and 30 days are shown in *Table 6*.

Analysis on polished mild steel showed an absence of chlorine and oxygen particles demonstrating the surface was absolutely free from any oxide layer and/or corroded particles. Similar phenomena were also observed after 3 hr of immersion. The absence of chlorine and oxygen atoms in this experiment could be attributed to slow corroding or adsorption processes and the formation of protective layer was still incomplete. After 30 days of exposure in the test solutions, a remarkable increase of chlorine and oxygen contents for mild steel coupons in blank solution was observed. The increase of these values could be associated with the formation of $FeCl_2$, $Fe(OH)_2$, Fe_2O_3, and/or Fe_3O_4 resulting from the attack of OH^- and Cl^- ion towards Fe^{2+}. Nevertheless, the presence of CPH has reduced chlorine and oxygen contents signifying possible occurrence of inhibitory activities of CPH on the mild steel surface. High content of Fe is commonly correlated to better inhibition behaviour. Meanwhile, mild steel severely corroded in blank solution giving very low value of Fe content.

Mechanism of Inhibition

Corrosion inhibition by CPH on mild steel is accomplished by adsorption of the CPH molecules on the mild steel surface followed by formation of a protective layer. In 1 M hydrochloric acid solution without inhibitor, Cl^- ion adsorbs on the mild steel surface to form chloro-complex at anode as follows (Yurt *et al*., 2004):

$$Fe + Cl^- \longleftrightarrow FeCl^-_{ads} \quad (i)$$
$$(FeCl^-)_{ads} \longrightarrow (FeCl_{ads})_+ + e \quad (ii)$$
$$(FeCl^+)_{ads} \longrightarrow Fe^{2+} + Cl^- \quad (iii)$$

Meanwhile, the cathodic hydrogen evolution follows these steps:

$$Fe + H^+ \longleftrightarrow (FeH^+)_{ads} \quad (iv)$$
$$(FeH^+)_{ads} + e \longrightarrow (FeH)_{ads} \quad (v)$$
$$(FeH)_{ads} + H^+ + e \longrightarrow Fe + H_2(g) \quad (vi)$$

In inhibited 1 M hydrochloric acid solution, $(FeCl^-)_{ads}$ form Fe-inhibitor complexes as follows:

$$(FeCl^-)_{ads} + Inhibitor \longleftrightarrow (FeCl\text{-}Inhibitor)_{ads} \quad (vii)$$
$$(FeCl\text{-}Inhibitor)_{ads} \longrightarrow (FeInhibitor)_{ads} + Cl^- \quad (viii)$$

In general, two modes of adsorption could be considered. Firstly, the neutral CPH molecules may adsorb the mild steel surface on the basis of donor-acceptor interactions between π-electrons and vacant *d*-orbitals of surface iron or also known as chemisorption. Furthermore, the double bonds also permit back donation of metal *d* electrons to the π^* orbital of inhibitor (Nasser and Sathiq, 2017). The unshared pair of electrons at *N* and O atoms also participate in making coordinate bonds with the mild steel surface. Secondly, the inhibitor may be adsorbed through physisorption in which Cl^- ions adsorb on the positively charged metal surface and create an excess of negative charges. Hence, protonated CPH molecules have high tendency to adsorb onto the mild steel surface thus reducing the dissolution of Fe to Fe^{2+}.

CONCLUSION

CPH acts as appreciably good inhibitor on mild steel in 1 M hydrochloric acid solution. Inhibition efficiencies noticeably increased with increasing inhibitor concentration and temperature. The polarisation study indicates that CPH function as a mixed-type corrosion inhibitor with a predominant control on anodic metal dissolution reaction. The inhibition efficiency, $\eta_{Tafel}(\%)$ calculation from Tafel analysis showed that the value approached 95% in the presence of 200 mg litre^{-1} CPH at 328K. The adsorption of CPH on mild steel surface obeyed the Langmuir adsorption isotherm through both physisorption and chemisorption. SEM micrographs clearly revealed that a change in the surface characteristics of the metal surface was due to the inhibition activity by CPH and this finding is supported by EDX data. The inhibition efficiencies obtained from polarisation and impedance analyses are in reasonably good agreement.

ACKNOWLEDGEMENT

The authors would like to thank the Director-General of MPOB for permission to publish this article. The authors also thank Sapiah Hashim and Mohd Zambri Yusof for their technical assistance.

REFERENCES

Amin, M A; Abd El-Rehim, S S; El-Sherbini, E E F and Bayyomi, R S (2007). The inhibition of low carbon steel corrosion in hydrochloric acid solutions by succinic acid: Part I. Weight loss, polarisation, EIS, PZC, EDX and SEM studies. *Electrochim. Acta, 52*: 3588-3600.

Bahrami, M J and Hosseini, S M A (2012). Electrochemical and thermodynamic investigation of the corrosion behaviour of mild steel in 1 M HCl solution containing organic compounds. *Int. J. Industrial Chemistry, 3*: 30 pp.

Banerjee, G and Malhotra, S N (1992). Contribution to adsorption of aromatic amines on mild steel surface from HCl solutions by impedance, UV and raman spectroscopy. *Corrosion, 48*: 10-15.

Bentiss, F; Lebrini, M; Lagrenee, M; Traisnel, A; Elfarouk and Vezin, H (2007). The influence of some new 2,5-disubstituted 1,3,4-thiadiazoles on the corrosion behaviour of mild steel in 1 M HCl solution. AC impedence study and theoretical approach. *Electrochim. Acta, 52*: 6865-6872.

Bentiss, F; Lebrini, M; Vezin, H; Chai, F; Traisnel, M and Lagrené, M (2009). Enhanced corrosion resistance of carbon steel in normal sulfuric acid medium by some macrocyclic polyether compounds containing a 1,3,4-thiadiazole moiety: AC impedance and computational studies. *Corros. Sci., 51*: 2165-2173.

Chakravarthy, M P and Mohana, K N (2014). Adsorption and corrosion inhibition characteristics of some nicotinamide derivatives on mild steel in hydrochloric acid solution. *ISRN Corrosion.* Article ID 687276.

Chitra, S; Parameswari, K and Selvaraj, A (2010). Dianiline schiff bases as inhibitors of mild steel corrosion in acid media. *Int. J. Electrochem. Sci*., *5*: 1675-1697.

Desai, M N; Desai, M B; Shah, C B and Desai, S M (1986). Schiff bases as corrosion inhibitors for mild steel in hydrochloric acid solutions. *Corros. Sci*., *26*: 827-837.

Diblíková, L; Jenípek, V; Hradec, P; Valeš, M and Szelag, P (2014). Mechanical and electrochemical evaluation of organic inhibitors effect on mild steel damage by hydrogen. *Procedia Engineering, 74*: 203-308.

Durnie, W H; Kinsella, B J; De Marco, R and Jefferson, A (2001). A study of the adsorption properties of commercial carbon dioxide corrosion inhibitor formulations. *J. Electrochem. Soc., 31*: 1221-1226.

Ehsani, A; Mahjani, M G; Moshrefi, R; Mostaanzadeh, H and Shayeh, J S (2014). Electrochemical and DFT study on the inhibition of 316L stainless steel corrosion in acidic medium by 1-(4-nitrophenyl)-5-amino-1H-tetrazole. *RSC Adv*., *4*: 20031-20037.

El-Lateef, H M A (2015). Experimental and computational investigation on the corrosion inhibition characteristics of mild steel by some novel synthesised imines in hydrochloric acid solutions. *Corros. Sci., 92*: 104-117.

El-Maksoud, S A A (2008). The effect of organic compounds on the electrochemical behaviour of steel in acidic media. A review. *Int. J. Electrochem. Sci., 3*: 528-555.

Ghazoui, A; Saddik, R; Bencat, N; Hammouti, B; Guenbour, M; Zarrouk, A and Ramdani, M (2012). The role of 3-amino-2-phenylimidazo[1,2-a] pyridine as corrosion inhibitor for C38 steel in 1 M HCl. *Der Pharma Chem., 4*: 352-364.

Hamdy, A and El-Gendy, N S (2013). Thermodynamic, adsorption and electrochemical studies for corrosion inhibition of carbon steel by henna extract in acid medium. *Egypt. J. Petrol., 22*: 17-25.

Karthikaiselvi, R and Subhashini, S (2014). Study of adsorption properties and inhibition of mild steel corrosion in hydrochloric acid media by water soluble composite poly(vinyl alcohol-o-methoxy aniline). *J. Assoc. Arab Univ. Basic Appl., 16*: 74-82.

Keersmaecker, M D; Depla, D; Verbeken, K and Adriaens, A (2014). Electrochemical and surface study of neutralized dodecanoic acid on a lead substrate. *J. Electrochem Soc*., *161*: C126-C137.

Kushairi, A; Loh, S K; Azman, I; Hishamuddin, E; Ong-Abdullah, M; Izuddin, Z B M N; Razmah, G; Sundram, S and Parveez, G K A (2018). Oil palm economic performance in Malaysia and R&D progress in 2017. *J. Oil Palm Res. Vol. 30(2)*: 163-195.

Li, S; Chen, S; Lei, S; Ma, H; Yu, R and Liu, D (1999). Investigation on some Schiff bases as HCl corrosion inhibitors for copper. *Corros. Sci., 41*: 1273-1287.

Li, W H; He, Q; Zhang, S T; Pei, C L and Hou, B R (2008). Some new triazole derivatives as inhibitors for mild steel corrosion in acidic medium. *J. Appl. Electrochem., 38*: 289-295.

Li, X; Deng, S; Fu, H and Mu, G (2009). Inhibition effect of 6-benzylaminopurine on the corrosion of cold rolled steel in H_2SO_4 solution. *Corros. Sci*., *51*: 620-634.

Mishra, M; Tiwari, K; Mourya, P; Singh, M M and Singh, V P (2015). Synthesis, characterisation and

corrosion inhibition property of nickel(II) and copper(II) complexes with some acylhydrazine Schiff bases. *Polyhedron, 89*: 29-38.

Mohd, N K; Ghazali, M; Yeong, S K; Ibrahim, N; Yunus, W M Z W; Nor, S M M and Idris, Z (2017). Corrosion inhibition of mild steel in hydrochloric acid solution using fatty acid derivatives. *J. Oil Palm Res*. *Vol. 29(1)*: 97-109.

Nasser, A J A and Sathiq, M A (2017). Comparative study of *N*-[(4-methoxyphenyl) (morpholin-4-yl) methyl]acetamide (MMPA) and N-[morpholin-4-yl(phenyl)methyl]acetamide (MPA) as corrosion inhibitors for mild steel in sulfuric acid solution. *Arab J. Chem., 10*: S261-S273.

Negm, N A; Ghuiba, F M and Tawfik, S M (2011). Novel isoxazolium cationic Schiff base compounds as corrosion inhibitors for carbon steel in hydrochloric acid. *Corros. Sci., 53*: 3566-3575.

Özcan, M; Karadag, F and Dehri, I (2008). Investigation of adsorption characteristics of methionine at mild steel/sulfuric acid interface: An experimental and theoretical study. *Colloids Surf A Physicochem Eng. Asp., 325*: 57-63.

Paul, A; Joby Thomas, K; Raphael, V P and Shaju, K S (2012). 3-Formylindole-4-aminobenzoic acid: A potential corrosion inhibitor for mild steel and copper in hydrochloric acid media. *ISRN Corrosion.* Article ID 842836.

Rafiquee, M Z A; Saxena, N; Khan, S and Quraishi, M A (2007). Some fatty acid oxadiazoles for corrosion inhibition of mild steel in HCl. *Indian J. Chem. Technol., 14*: 576-583.

Ramesh, S V and Adhikari, V (2007). Inhibition of corrosion of mild steel in acid media by N′-benzylidene-3-(quinolin-4-ylthio) propanohydrazide. *Bull. Mater. Sci., 31*: 699-709.

Ramya, K; Mohan, R; Anupama, K K and Joseph, A (2015). Electrochemical and theoretical studies on the synergistic interaction and corrosion inhibition of alkyl benzimidazoles and thiosemicarbazide pair on mild steel in hydrochloric acid. *Mater. Chem. Phys., 149-150*: 632-647.

Rivera-Grau, L M; Casales, M; Regla, I; Ortega-Toledo, D M; Ascencio-Gutierrez, J A and Martinez-Gomez, L (2013). Effect of organic corrosion inhibitors on the corrosion performance of 1018 carbon steel in 3% NaCl solution. *Int. J. Electrochem. Sci., 8*: 2491-2503.

Roy, P; Karfa, P; Adhikari, U and Sukul, D (2014). Corrosion inhibition of mild steel in acidic medium by polyacrylamide grafted Guar gum with various grafting percentage: Effect of intramolecular synergism. *Corros. Sci., 88*: 246-253.

Safak, S; Duran, B; Yurt, A and Türkoğlu, G (2012). Schiff bases as corrosion inhibitor for aluminium in HCl solution. *Corros. Sci., 54*: 251-259.

Sakunthala, P; Vivekananthan, S S; Gopiraman, M; Sulochana, N and Vincent, A R (2013). Spectroscopic investigations of physicochemical interactions on mild steel in an acidic medium by environmentally friendly green inhibitors. *J. Surfactants Deterg., 16*: 251-263.

Shahin, M; Bilgic, S and Yilmaz, H (2003). The inhibition effects of some cyclic nitrogen compounds on the corrosion of the steel in NaCl medium. *Appl. Surf. Sci., 195*: 1-7.

Sigircik, G; Tunc Tüken and Mehmet Erbil, M (2016). Assessment of the inhibition efficiency of 3,4-diaminobenzonitrile against the corrosion of steel. *Corros. Sci., 102*: 437-445.

Singh, A K and Quraishi, M A (2012). Study of some bidentate Schiff bases of isatin as corrosion inhibitors for mild steel in hydrochloric acid solution. *Int. J. Electrochem. Sci*., 7: 3222-3241.

Solmaz, R; Kardas, G; Culha, M; Yazici, B and Erbil, M (2008). Investigation of adsorption and inhibitive effect of 2-mercaptothiazoline on corrosion of mild steel in hydrochloric acid media. *Electrochim. Acta, 53*: 5941-5952.

Su, X; Lai, C; Peng, L; Zhu, H; Zhou, L; Zhang, L; Liu, X and Zhang, W (2016). A dialkyldithiophosphate derivative as mild steel corrosion inhibitor in sulfuric acid solution. *Int. J. Electrochem. Sci., 11*: 4828-4839.

Tan, Y J; Bailey, S and Kinsellal, B (1996). An investigation of the formation and destruction of corrosion inhibitor films using electrochemical impedance spectroscopy (EIS). *Corros. Sci., 38*: 1545-1561.

Tawfik, S M and Zaky, M F (2015). Corrosion inhibition performance of some Schiff base anionic surfactant complexes of cobalt(II), copper(II), and zinc(II) on carbon steel in 1.0 M HCl. *Res. Chem. Intermediat., 41*: 8747-8772.

Verma, C B and Quraishi, M A (2014). Schiff's bases of glutamic acid and aldehydes as green corrosion inhibitor for mild steel: Weight-loss, electrochemical

and surface analysis. *Int. J. Innov. Res. Sci. Eng. Technol.*, *3*: 14501-14613.

Yurt, A; Balaban, A; Ustün Kandemir, S; Bereket, G and Erk, B (2004). Investigation on some Schiff bases as HCl corrosion inhibitors for carbon steel. *Mater. Chem. Phys.*, *85*: 420-426.

Zarrouk, A; Hammouti, B; Zarrok, H; Al-Deyab, S S and Messali, M (2011). Temperature effect, activation energies and thermodynamic adsorption studies of l-cysteine methyl ester hydrochloride as copper corrosion inhibitor in nitric acid 2 M. *Int. J. Electrochem. Sci.*, *6*: 6261-6274.